

Physicochemical Properties and Fracture Behavior of Soy-Based Resin

A. Shabeer, S. Sundararaman, K. Chandrashekhara, L. R. Dharani

Department of Mechanical and Aerospace Engineering, University of Missouri—Rolla, Rolla, Missouri 65409

Received 20 November 2006; accepted 6 February 2007

DOI 10.1002/app.26322

Published online 28 March 2007 in Wiley InterScience (www.interscience.wiley.com).

ABSTRACT: A soy-based resin was prepared by the process of transesterification and epoxidation of regular food-grade soybean oil. The soy-based resin was used as a reactive diluent and also as a replacement of bisA epoxy resin in an anhydride-cured polymer. The curing efficiency of soy epoxy resin was studied using differential scanning calorimetry. Physicochemical properties and fracture behavior of soy-based resin polymers were studied using dynamic mechanical analysis and fracture toughness measurements, respectively. Toughness measurements were carried out using the compact tension geometry following the principles

of linear elastic fracture mechanics. Tests showed that the addition of soy-based epoxy resin to the base epon resin improved the toughness of the blend. Morphology of the fractured specimens has been analyzed by scanning electron microscopy. The soy-based resins hold great potential for environmentally friendly, renewable resource based, and low cost materials for structural applications. © 2007 Wiley Periodicals, Inc. *J Appl Polym Sci* 105: 656–663, 2007

Key words: soy resin; fracture toughness; crosslinking density

INTRODUCTION

The fatty acid esters derived from the triglyceride vegetable oils are an attractive source of raw materials for polymer synthesis. Among the triglyceride oils, soybean attracts great interest because of its plentiful supply in the United States, relatively low cost, and environmentally benign properties. Soybean oil contains 85% unsaturated oleic, linoleic and linolenic fatty acids.^{1,2} This high degree of unsaturation makes it possible to polymerize the oil into useful materials. The carbon–carbon double bonds can be epoxidized to form reactive groups, which are capable of forming a crosslinking polymer network structure.³

Many researchers have attempted to use epoxidized soybean oil (ESO) for polymeric and composite applications. However, because of low reactivity of internal epoxy groups and a tendency for intramolecular bonding, ESO normally has a low crosslinking density and therefore limited thermal and mechanical properties. Most ESO industrial applications are still limited to nonstructural applications such as coatings.⁴

In a previous study, a soy-based epoxy resin system utilizing epoxidized allyl soyate (EAS) was synthesized by blending EAS with bisphenol A epoxy resin.^{5,6} EAS resin has proved to be chemically flexible and it tends to improve some of the mechanical properties.

The fracture behavior of epoxy resins is of considerable importance to ensure performance of these materials in structural components in housing, aircraft, and automobiles. All the aforementioned applications require the structural material to be tough to bear the load. However, most of the commercially available epoxy resins are brittle with low strain to failure.⁷ To enhance the toughness of the epoxy resins, several methods such as incorporating rubber particles into the base resin were employed, where the dispersed rubber phase plays a considerable part in the toughening effect.⁸ However, these toughened epoxies exhibit rather low glass transition temperature (T_g), low crosslinking densities, and also lead to poorer thermal stability of the resin.

Studies have also shown that the toughening effect in the rubber-modified epoxy resins may be attributed to the rubber stretching and tearing.^{9,10} More recently, it was reported that the toughening in rubber-modified epoxy systems was due to the cavitation of rubber particles followed by shear yielding of the epoxy matrix.^{11,12} The shear yielding of the epoxies depends on the crosslinking density and the T_g . Thus, epoxies with low crosslinking density can be easily toughened because of more shear yielding. However, the use of rubbers such as

Correspondence to: K. Chandrashekhara (Chandra@umr.edu).

Contract grant sponsor: National Science Foundation; contract grant number: NSF CMS-0533201.

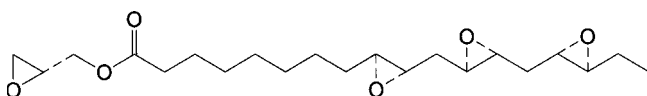


Figure 1 Structure of soy epoxy resin.

carboxyl-terminated butadiene acrylonitrile and amine-terminated butadiene acrylonitrile to improve the toughness of the epoxy resins has resulted in a reduction in thermal and mechanical properties.¹³

Attempts to enhance the fracture toughness of the epoxy using thermoplastic additives and organic fillers have resulted in the material having poor resistance to solvents and weak chemical bonding.¹⁴ But thermoplastic additives have been found to be more effective than rubber particles in enhancing the toughness.¹⁵ Suebert et al.¹⁶ also demonstrated the idea of adding liquid rubber with unsaturated polyester systems.

Recently, toughening agents with functional groups were added to increase the toughness of epoxy resins. The results showed that the maximum fracture toughness can only be obtained when the optimum amount of functional groups is introduced.¹⁷ Research is also being carried out to improve the toughness of rigid epoxy networks using vegetable-oil-based polymeric materials. The resins obtained using the vegetable oils are more flexible because of the presence of long carbon chains.^{18,19}

There have also been investigations on the effect of crosslinking density on the fracture toughness of the epoxy.²⁰ The general trend is that fracture toughness decreased with increase in crosslinking density. Plangsangmas et al.²¹ also showed the direct dependence of fracture toughness on the molecular weight between crosslinks (M_c). Lower M_c values resulted in a network with high rigidity, which reduced the degree of energy dissipation at the crack tip.²²

Min et al.²³ reported that free volume, chain flexibility, and intermolecular packing were more dominant than crosslinking density in deciding the fracture behavior of diglycidyl ether of bisphenol A crosslinked with diamino diphenyl sulfone. Gupta et al.²⁴ reported that intermolecular packing, molecular architecture, and molar mass affected the fracture toughness below the T_g of the resins. The T_g also plays a significant part in the fracture behavior of

TABLE I
Compositions of the Soy Epoxy Anhydride Polymer

Sample	Epon 9500 (gm)	EAS (gm)	LS 56 (gm)
Pure Epon	100	0	70
25% EAS	75	25	70
50% EAS	50	50	70
75% EAS	25	75	70

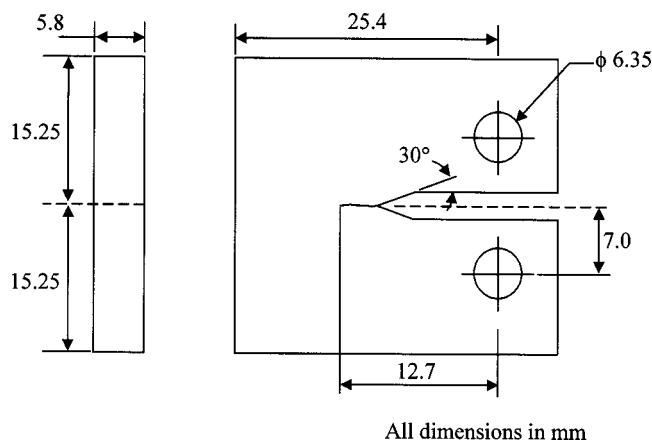


Figure 2 Fracture specimen.

epoxy resins.²⁵ Hence it is also important to understand the role of T_g on the toughness of the epoxy resins. The T_g of the epoxy networks was found to increase as M_c decreased. Fox and Loshaek²⁶ showed that T_g increased as molecular weight between crosslinks decreased for both the trifunctional and tetrafunctional epoxy networks. Bank and Ellis²⁷ have proposed a linear relationship between the T_g and $1/M_c$ using network free volume theory.

In the present work, soy-based resins were characterized through physicochemical properties and fracture toughness measurements. The physicochemical properties of the soy-based resins were investigated using dynamic mechanical analysis (DMA). The curing mechanisms with the different amounts of soy resin were studied using differential scanning calorimetry. Fracture toughness tests were carried out using compact tension geometry. The morphology of the fractured surfaces was observed by scanning electron microscopy (SEM).

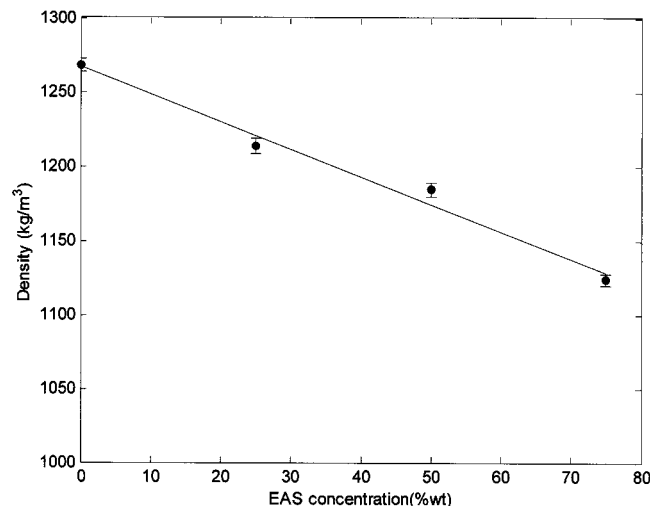


Figure 3 Variation of density with soy resin concentration.

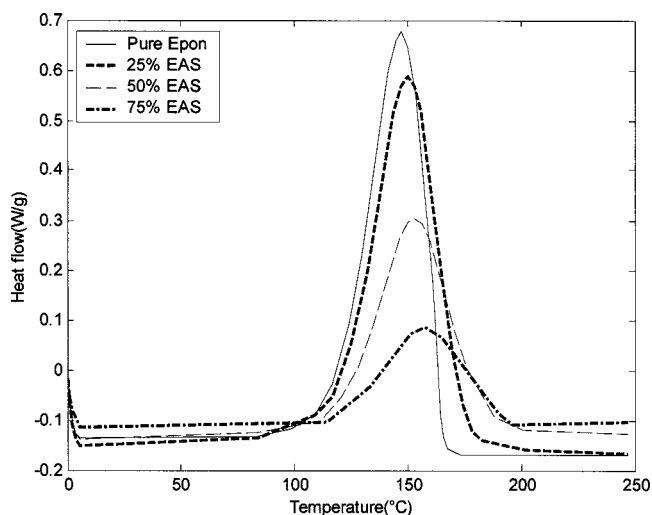


Figure 4 Dynamic curing curves of soy epoxy anhydride polymers.

EXPERIMENTAL

Materials

The base epoxy resin used in the study was Shell Epon[®] 9500 (Shell Chemical Co., Houston, TX) with an epoxide equivalent weight of 175–190. Lindride[®] LS 56V (Lindau Chemicals, Columbia, SC) was the anhydride curing agent used. The soy-based resin reactive diluent was synthesized in a two-step laboratory scale process from regular food-grade soybean oil. At first, the triglyceride molecules in the soybean oil were transesterified with allyl alcohol to yield fatty acid allyl esters. Next, the fatty acid esters were epoxidized using benzoyl peroxide to yield soyate epoxy resin. The chemical structure of soy epoxy resin is shown in Figure 1.

Preparation of soy-based epoxy resin

The blends were prepared by mixing the soy epoxy resin with the base bisphenol A epoxy resin. The weight ratios of soy epoxy resin to Epon resin blend chosen for the present work were 75 : 25, 50 : 50, 25 : 75, and 0 : 100, as shown in Table I.

Next, curing agent was added to the epoxy resin blend. The resin and the hardener were mixed well. The mixture was degassed for a few minutes to

remove any air bubbles. The mixture was poured into a preheated mold, which had been sprayed with a mold release agent, Chemlease[®] 41 (Chem-Trend Incorporated, Howell, MI). Curing was performed in the oven in two stages to remove air bubbles from the resin samples. First, the mixtures were cured for 1 h at 80°C and then followed by curing for 1.5 h at 175°C.

Density measurement

The density of the soy-based epoxy was determined by the displacement method according to ASTM D 792-91. The liquid used for displacement was distilled water. The dimensions of the samples were 10 mm × 10 mm × 5 mm. Five samples of each type were measured.

Differential scanning calorimetry

Differential scanning calorimetry (DSC) testing was performed on TA Instrument model 2100. The samples (10–14 mg) of soy-based epoxy resin-curing agent were placed into an aluminum crucible. The resin samples were cured at a rate of 10°C/min from 30 to 250°C. The onset of cure and end of cure were measured for each sample. The onset and end of cure are defined as the points of intersection of the tangent drawn at the points of greatest slope on the curing curve with the extrapolated baseline prior and following the transition respectively. Once the samples were cured in the DSC, the cell was quickly cooled using liquid nitrogen and subjected to subsequent scanning from –50 to 120°C to measure the resulting T_g . The T_g was reported as the inflection point of the glass transition region.

Dynamic mechanical analysis

The dynamic mechanical tests were performed using a Perkin-Elmer DMA Pyris-7e analyzer. Data were collected and analyzed using Pyris software. The specimens were deformed under a three-point flexural mode arrangement. Rectangular specimens 23 mm in length and 5 mm × 5 mm in cross section were used. The tests were carried out in a fixed frequency mode in which the frequency was held constant at 1 Hz and the temperature was ramped

TABLE II
Differential Scanning Calorimetry Results

Sample	T_{onset} (°C)	T_{midpoint} (°C)	T_{end} (°C)	T_g (°C)	Heat of reaction (H) (J/g)
Pure Epon	70.17	146	170.32	89.5	187
25% EAS	74.3	148.5	203.74	78	146.3
50% EAS	94.6	151.3	210.67	67.3	120.7
75% EAS	102.4	162.8	215.48	41.7	113

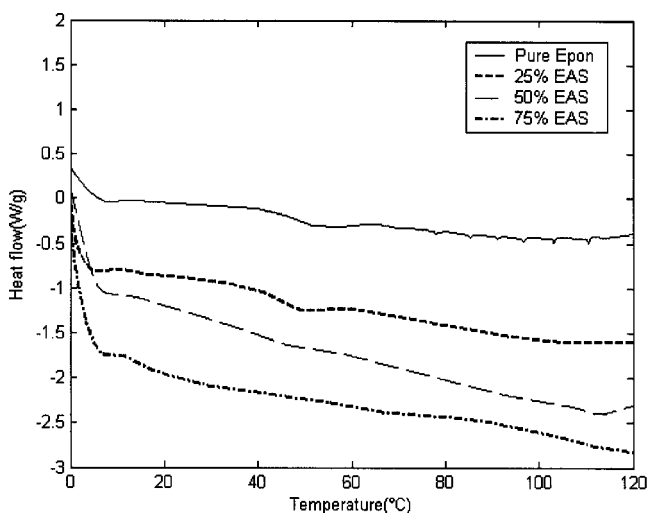


Figure 5 DSC thermograms showing the glass transition region of soy epoxy anhydride polymers.

from 0 to 150°C at a heating rate of 5°C/min, The loss factor ($\tan \delta$), storage modulus, and loss modulus were plotted as a function of temperature. The T_g of the resins was obtained from the peaks of the $\tan \delta$ curves. A minimum of three specimens of each composition were tested.

Fracture testing

The fracture toughness tests was carried out on a compact tension (CT) specimens as per ASTM D 5045 on a MTS 810 hydraulic testing machine equipped with 458.20 Micro console, M58.91 Micro profiler and 458.11 controllers for load and stroke. The specimen dimensions are shown in Figure 2. All the tests were performed at a cross head velocity of 10 mm/

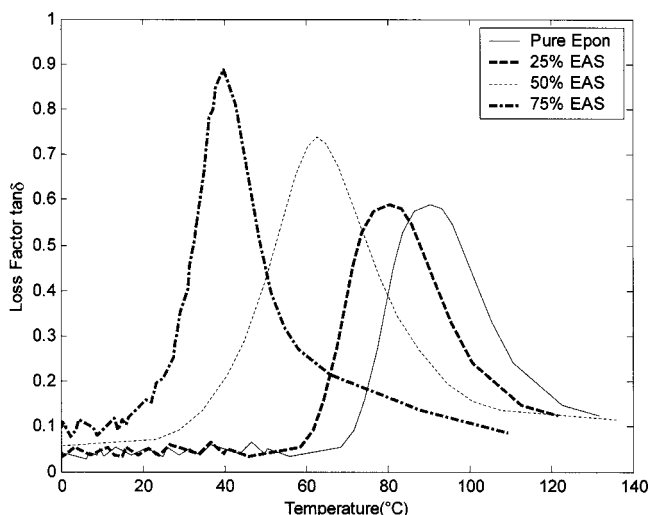


Figure 6 Loss factor ($\tan \delta$) curves of soy epoxy anhydride polymers.

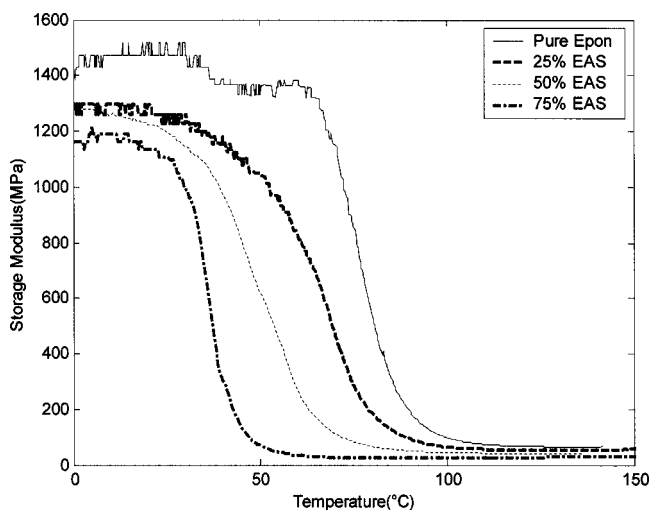


Figure 7 Storage modulus curves of soy epoxy anhydride polymers.

min. Precracks were made in the specimens with the help of a jeweler’s saw. At least five specimens were used for each different resin system and the average measurements are reported with corresponding error bars at ± 1 standard deviation from the mean. The following relationship was used to calculate the plain strain fracture toughness (K_{1C}) of the compact specimen.

$$K_{1C} = \frac{P_Q}{bw^{1/2}}f(x), \tag{1}$$

where P_Q is the critical load obtained from the load-deflection curve, w is the width, b is the specimen thickness, and $f(x)$ is the dimensionless function dependant on specimen geometry.

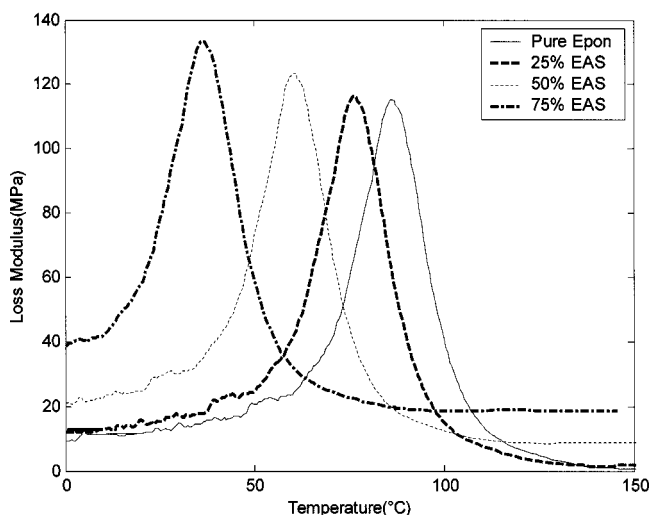


Figure 8 Loss modulus curves of soy epoxy anhydride polymers.

TABLE III
Dynamic Mechanical Properties of Soy Epoxy Anhydride Polymer at Room Temperature and Rubbery Plateau Region

Sample	Storage modulus (E') (MPa)		Loss modulus (E'') (MPa)	
	At 30°C	At 130°C	At 30°C	At 130°C
Pure Epon	1470 ± 26.8	67 ± 5.8	14.8 ± 11.67	2.04 ± 3.25
25% EAS	1260 ± 72.15	54.7 ± 3.23	17.2 ± 17.83	2.1 ± 1.42
50% EAS	1140 ± 34.56	41.1 ± 7.92	30.1 ± 30.76	8.72 ± 3.94
75% EAS	983 ± 23.6	26.8 ± 2.64	108 ± 24.85	18.8 ± 5.87

Scanning electron microscopy

Fracture surfaces of different soy-based epoxy specimens were analyzed using scanning electron microscope (SEM) JEOL T330. An accelerating voltage of 10 kV was used to collect images for all the samples. Before testing, samples were coated with a thin layer of gold to improve the conductivity and to prevent surface charging.

RESULTS AND DISCUSSION

Density of soy-based epoxy resin

Figure 3 shows the density of the soy epoxy anhydride polymer. The density of the soy-based epoxy anhydride polymer decreased with increasing amount of soy resin. The solid line represents the least-squares fit line of the data.

Differential scanning calorimetry

Figure 4 shows the DSC measured exotherm data of soy epoxy anhydride polymers. Table II summarizes the DSC results. The DSC exotherms showed that an increase of the soy resin concentration caused a shift in the exotherm peak maximum toward lower values. The onset temperature of curing and the temperature of the peak exothermal heat for the bisphenol A epoxy resin were 70.2 and 146°C, respectively, whereas they were 74.3 and 148.5°C for the 25% soy epoxy resin, 94.6 and 151.3 °C for the 50% soy epoxy resin and 102.4 and 162.8°C for the 75% soy epoxy resin, respectively. These results

demonstrated that the onset temperature for curing and the temperatures of maximum exotherm heat shifted to higher temperatures for soy epoxy resin when compared with pure bisphenol A epoxy resin. The possible explanation can be due to presence of less reactive internal epoxy groups present in soy epoxy resin. It can also be seen that the heat of reaction was reduced upon an increase in concentration of soy resin.

Figure 5 shows the glass transition curves of the soy epoxy anhydride polymer. A decrease in T_g with increasing concentration of soy resin was observed in this study. The decrease in T_g can be due to reduced crosslinking density of the polymeric network. Hence, soy epoxy anhydride polymers require more curing agent or a more efficient curing agent to maximize crosslinking of the epoxy anhydride polymer matrix.

Dynamic mechanical analysis

DMA has been used to evaluate the damping characteristics of polymers and rubbers. It has proved to be an effective tool in the characterization of viscoelastic materials. It measures the response of a material as it is deformed due to a sinusoidal stress for a wide range of temperatures and frequencies. The dynamic mechanical properties such as storage modulus (E'), loss modulus (E''), and the mechanical loss factor ($\tan \delta$) of soy epoxy anhydride polymer were evaluated from 0 to 150°C. Figure 6 shows the temperature dependence of loss tangent of soy epoxy anhydride polymer. The loss tangent peak

TABLE IV
Crosslinking Density, Molecular Weight between Crosslinks, and Glass Transition Temperature of Soy Epoxy Anhydride Polymer

Sample	Crosslinking density, ν_e (mol/m ³)	Molecular weight between crosslinks, M_c (g/mol)	Glass transition temperature, T_g (°C) (from loss tangent curves)
Pure Epon	6426	198	90
25% EAS	5412	224	81
50% EAS	4019	295	66
75% EAS	2805	401	40.5

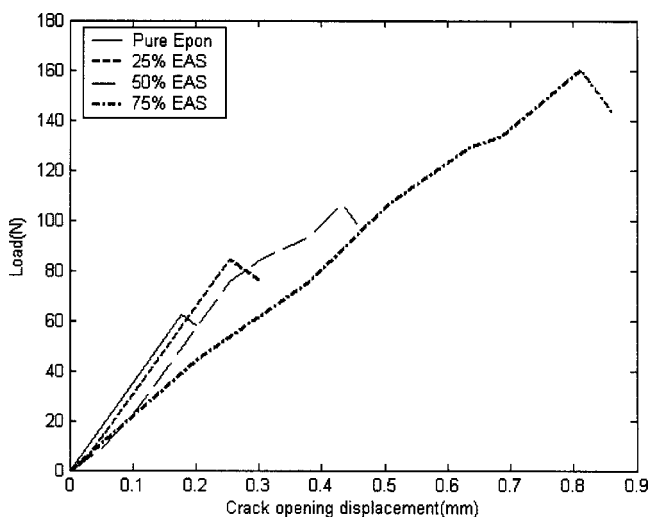


Figure 9 Load versus crack opening displacement of soy epoxy anhydride polymer.

increased with the increase in soy resin concentration and also the peak shifted towards lower temperatures. The loss tangent peak is associated with the molecular movement of polymeric chains within the structure where higher the peak $\tan \delta$ value, the greater the mobility of polymeric chains. Comparing the peaks in Figure 6, it can be seen that the 75% EAS has the highest $\tan \delta$ value, indicating the most molecular mobility. The T_g obtained from the peak position of the loss tangent curve decreased with the addition of soy resins. Also, the appearance of single relaxation peak in the loss tangent curve indicated the presence of single, homogenous phase at the molecular level.

Figures 7 and 8 show the change of storage and loss modulus of the soy epoxy anhydride polymer,

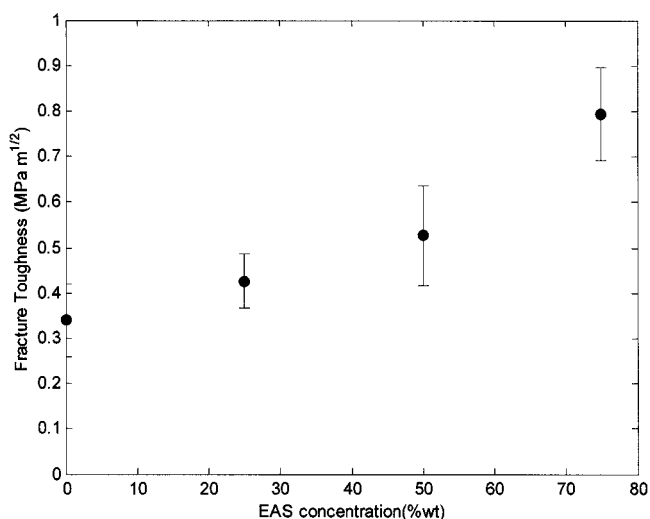


Figure 10 Variation of fracture toughness with concentration of soy epoxy anhydride polymer.

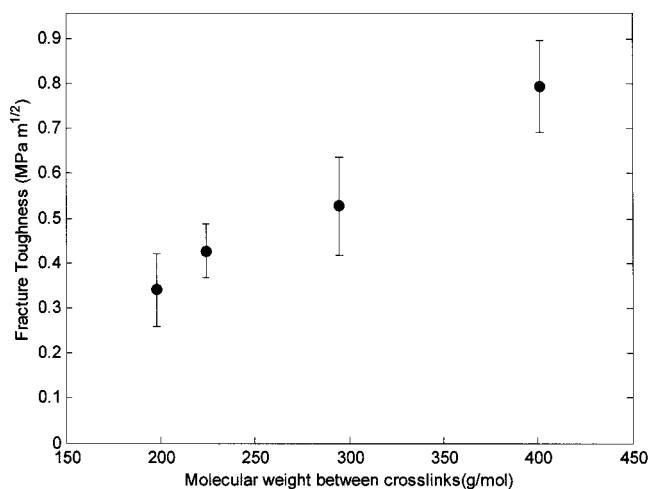


Figure 11 Variation of fracture toughness with the molecular weight between crosslinks.

respectively. The storage modulus initially remained constant at lower temperatures. As the temperature increased into the glass transition, the storage modulus exhibited a sharp drop, which was followed by a modulus plateau at higher temperatures. Table III shows the storage modulus at 30 and 130°C. Storage modulus of soy epoxy anhydride polymer at temperatures lower than the T_g decreased with increasing amount of soy resin concentration. Thus, the 75% EAS possessed the lowest storage modulus over the entire temperature region studied.

From the theory of rubber elasticity, the crosslinking density (ν_e) of a crosslinked polymer can be determined by the following equation.^{27,28}

$$E' = 3\nu_e RT, \tag{2}$$

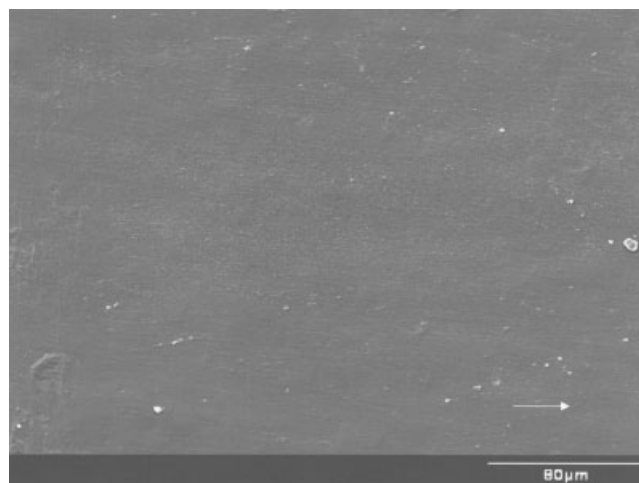


Figure 12 Scanning electron micrograph of pure bisphenol A epoxy resin.

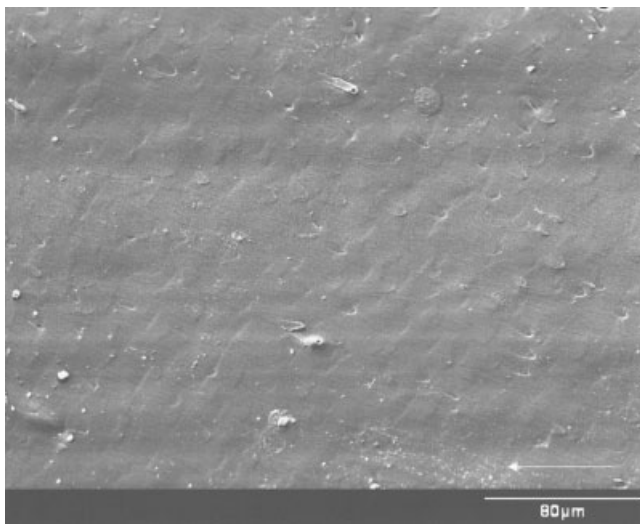


Figure 13 Scanning electron micrograph of 25% soy epoxy anhydride polymer.

where E' is the storage modulus in the rubbery plateau region, R is the gas constant, and T is the absolute temperature. Table IV shows the calculated crosslinking densities of the soy epoxy anhydride polymers when compared with the neat bisphenol A epoxy anhydride system. An increase in concentration of soy resin decreased the crosslinking density of the network.

The molar mass between crosslinks (M_c) can be similarly determined using the rubber elasticity theory based on the assumption that the network structure has sufficient molar mass and degree of flexibility to exhibit rubber elasticity.^{28,29}

$$E' = \frac{3\rho RT}{M_c}, \quad (3)$$

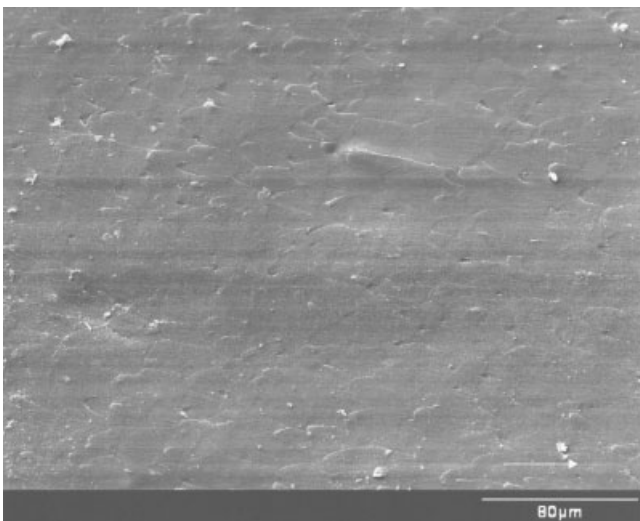


Figure 14 Scanning electron micrograph of 50% soy epoxy anhydride polymer.

where E' is the storage modulus in the rubbery plateau region, ρ is the polymer density, R is the gas constant, and T is the absolute temperature. Equation 3 can be applied to highly crosslinked materials such as epoxy after considering the finite extensibility of short network chains. Table IV shows the molecular weight between crosslinks of the soy epoxy anhydride polymer. Increase in concentration of soy resin increased the molecular weight between crosslinks of the network, which corresponds to the reduced crosslinking density. Figure 8 shows the temperature dependence of loss modulus of soy epoxy anhydride polymer. The peak of the loss modulus shifted to lower temperatures as the soy resin concentration increased in the epon resin. This is presumably due to the introduction of the more flexible fatty acid chain into the epoxy system. Table III reports the loss modulus measured at 30 and 130°C. Loss modulus of soy epoxy anhydride polymer increased with increasing amount of soy resin concentration.

Fracture testing

The fracture toughness measurements of resin samples were conducted based on the linear elastic fracture mechanics approach. The load versus crack opening displacement of soy epoxy anhydride polymer is shown in Figure 9. Figure 10 shows the fracture toughness of soy-based epoxy anhydride polymers. In general, with an increase in the soy resin concentration, the fracture toughness increased. With 75% of soy resin added to the base epon resin, an increase of the fracture toughness from 0.32 to 0.78 MPa m^{1/2} was observed. This increase in toughness can be attributed to the observed decrease in

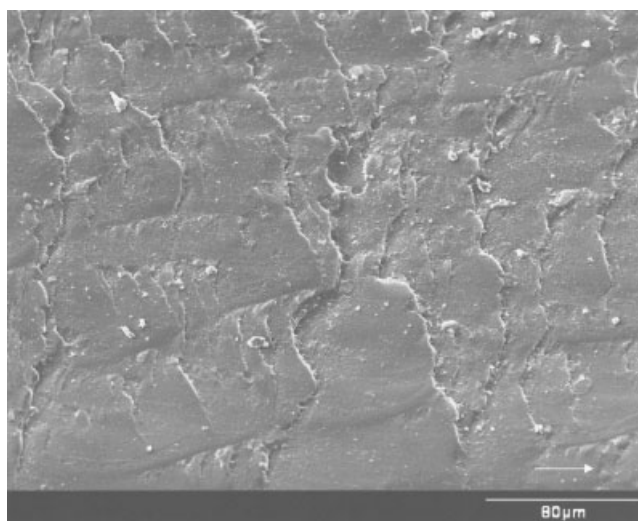


Figure 15 Scanning electron micrograph of 75% soy epoxy anhydride polymer.

the crosslinking density or the increase in the molecular weight between network crosslinks. The plot of K_{IC} versus M_c of soy-based epoxy anhydride polymer is illustrated in Figure 11. The fracture toughness increased with the increase in the molecular weight between crosslinks of the soy-based resins.

Figures 12–15 are the scanning electron micrographs showing fracture surfaces of soy-based epoxy anhydride polymer. Figure 12 shows the fracture surface of pure bisphenol A epoxy resin. The failure surface of pure bisphenol A epoxy resin was extremely flat and did not show crack arrest lines, suggesting that the pure bisphenol A epoxy resin was elastic rather than plastic and the crack was propagated with minimal hindrance. The surfaces of 25, 50, and 75% soy resin are shown in Figures 13, 14, and 15, respectively. The failure surfaces showed crack arrest lines, indicating the ductility of the polymer matrix. The crack tip for the 75% soy resin experienced more plastic deformation, thus arresting the crack propagation much more efficiently than the bisphenol A epoxy resin, resulting in enhanced fracture toughness.

CONCLUSIONS

The physicochemical properties and fracture behavior of novel soy-based epoxy resins were investigated. Addition of soy-based epoxy diluent produced a less glassy, more rubbery material that displayed the following. DSC plots showed that the addition of soy in the base bisphenol A epoxy resin shifted the onset of curing to higher temperatures and their curing evolved less exothermal heat. DMA showed that the addition of soy resin decreased the peak of loss tangent and shifted it to lower temperatures. Storage modulus decreased with increasing amount of soy resin. Crosslinking density, obtained from the rubber elasticity theory, was observed to decrease with the concentration of soy resin. The T_g of the polymer decreased with increasing soy resin content. This decrease in T_g was attributed to the reduced crosslinking densities of the epoxy polymers. The fracture toughness of soy epoxy anhydride polymer was greatly improved with the addition of soy resin concentration, from 0.35 MPa m^{1/2} for pure bisphenol A epoxy resin to 0.78 MPa m^{1/2} for 75% soy epoxy resin. The increase in fracture toughness of the blend was also attributed to lesser degree of crosslinking. Postfailure examination of fracture surfaces using microscopy indicated the

presence of ductile fracture at higher concentration of soy resin.

The authors thank Dr. Thomas Schuman of University of Missouri—Rolla for his helpful suggestions.

References

1. Nevin, C. S.; Moser, B. F. *J Appl Polym Sci* 1963, 7, 1853.
2. Kaplan, D. L. *Biopolymers from Renewable Resources*; Springer: New York, 1998.
3. Li, F.; Larock, R. C. *J Appl Polym Sci* 2000, 78, 1044.
4. Kumar, G. S. *Biodegradable Polymers: Prospects and Progress*; Marcel Dekker, New York, 1987.
5. Zhu, J.; Chandrashekhara, K.; Flanigan, V.; Kapila, S. *J Appl Polym Sci* 2004, 91, 3513.
6. Shabeer, A.; Garg, A.; Sundararaman, S.; Chandrashekhara, K.; Flanigan, V.; Kapila, S. *J Appl Polym Sci* 2005, 98, 1772.
7. Hung, J. S.; Garcia, E. I.; Pickelman, D. M. In *Polymer Toughening*; Arends, C. B., Eds.; Marcel Dekker: New York, 1996; Chapter 5.
8. Bascom, W. D.; Cottingham, R. L.; Jones, R. L.; Peyser, P. *J Appl Polym Sci* 1975, 19, 2545.
9. Argon, A. S.; Cohen, R. E. *Polymer* 2003, 44, 6013.
10. Azimi, H. R.; Pearson, R. A.; Hertzberg, R. W. *J Appl Polym Sci* 1995, 58, 449.
11. Kar, S.; Banthia, A. K. *J Appl Polym Sci* 2004, 92, 3814.
12. Fellahi, S.; Chikhi, N.; Bakar, M. *J Appl Polym Sci* 2001, 82, 861.
13. Lesser, A. J.; Kody, R. S. *J Polym Sci Part B: Polym Phys* 1997, 35, 1611.
14. Varley, R. J. *Polym Int* 2003, 53, 78.
15. Hourston, D. J.; Lane, J. M.; Zhang, H. X. *Polym Int* 1996, 42, 349.
16. Suebert, A. R.; Guiley, C. D.; Eplin, A. M. *Advances in Chemistry (Series No. 222)*; American Chemical Society: Washington, DC, 1989; p 389.
17. Harani, H.; Fellahi, S.; Bakar, M. *J Appl Polym Sci* 1999, 71, 29.
18. Frischinger, I.; Dirlikov, S. In *Toughened Plastics I. Advances in Chemistry (series no. 233)*; Reiw, C. K., Kinloch, A. J., Eds.; American Chemical Society: Washington, DC, 1993; 451.
19. Rosch, J.; Mulhaupt, R. *Polym Bull* 1993, 31, 679.
20. Cook, W. D. *J Appl Polym Sci* 1990, 42, 1259.
21. Plangsangmas, L.; Mecholsky, J. J.; Brennan, A. B. *J Appl Polym Sci* 1999, 72, 257.
22. Lesser, A. J.; Crawford, E. *J Appl Polym Sci* 1997, 66, 387.
23. Min, B. G.; Hodgkin, J. H.; Stachurski, Z. H. *J Appl Polym Sci* 1993, 48, 1303.
24. Gupta, V. B.; Drzal, L. T.; Lee, C. Y.; Rich, M. J. *Polym Eng Sci* 1985, 25, 812.
25. Liu, T.; Tjiu, W. C.; Tong, Y.; He, C.; Goh, S. S.; Chung, T. S. *J Appl Polym Sci*, 2004, 94, 1236.
26. Fox, T. G.; Loshaek, S. *J Polym Sci* 1955, 15, 371.
27. Banks, L.; Ellis, B. *Polymer* 1982, 23, 1466.
28. Nielson, L. E.; Landel, R. F. *Mechanical Properties of Polymers and Composites*, 2nd ed.; Marcel Dekker: New York, 1994.
29. Klemperer, D.; Sperling, L. H.; Utracki, L. A. *Interpenetrating Polymer Networks (ACS Symposium Series, No. 239)*; American Chemical Society: Washington, DC, 1994.